




RESEARCH ARTICLE

One drug-sensitive subunit is sufficient for a near-maximal retigabine effect in KCNQ channels

Michael C. Yau^{1,2} , Robin Y. Kim¹, Caroline K. Wang¹ , Jingru Li¹ , Tarek Ammar¹, Runying Y. Yang¹, Stephan A. Pless² , and Harley T. Kurata¹ 

Retigabine is an antiepileptic drug and the first voltage-gated potassium (Kv) channel opener to be approved for human therapeutic use. Retigabine is thought to interact with a conserved Trp side chain in the pore of KCNQ2–5 (Kv7.2–7.5) channels, causing a pronounced hyperpolarizing shift in the voltage dependence of activation. In this study, we investigate the functional stoichiometry of retigabine actions by manipulating the number of retigabine-sensitive subunits in concatenated KCNQ3 channel tetramers. We demonstrate that intermediate retigabine concentrations cause channels to exhibit biphasic conductance–voltage relationships rather than progressive concentration-dependent shifts. This suggests that retigabine can exert its effects in a nearly “all-or-none” manner, such that channels exhibit either fully shifted or unshifted behavior. Supporting this notion, concatenated channels containing only a single retigabine-sensitive subunit exhibit a nearly maximal retigabine effect. Also, rapid solution exchange experiments reveal delayed kinetics during channel closure, as retigabine dissociates from channels with multiple drug-sensitive subunits. Collectively, these data suggest that a single retigabine-sensitive subunit can generate a large shift of the KCNQ3 conductance–voltage relationship. In a companion study (Wang et al. 2018. *J. Gen. Physiol.* <https://doi.org/10.1085/jgp.201812014>), we contrast these findings with the stoichiometry of a voltage sensor-targeted KCNQ channel opener (ICA-069673), which requires four drug-sensitive subunits for maximal effect.

Introduction

Voltage-gated potassium channels encoded by the KCNQ gene family are subject to dual regulation by voltage and PIP₂ (Haley et al., 1998; Wang et al., 1998; Brown et al., 2007). In the central nervous system and certain sensory organs, KCNQ2–5 subunits encode the M-current, initially characterized as a hyperpolarizing potassium current sensitive to muscarinic signaling (Brown and Adams, 1980; Biervert et al., 1998; Charlier et al., 1998; Singh et al., 1998). Functional activity of KCNQ channels depends on the presence of adequate PIP₂ levels in the membrane (Suh et al., 2006; Suh and Hille, 2007). Activation of signaling cascades that deplete PIP₂, via M1-receptor activation or other G-protein-coupled receptors that signal through G_q and phospholipase C, lead to current reduction and consequently enhanced neuronal excitability (Brown and Passmore, 2009). KCNQ channels are also unique among the voltage-gated potassium channel family in that they are sensitive to a chemically diverse set of compounds that act as channel openers (Bentzen et al., 2006; Xiong et al., 2007, 2008; Miceli et al., 2008; Yu et al., 2011). Although a variety of compounds have been shown to exhibit KCNQ channel-activating properties, retigabine and its close analogue, flupirtine (used as an analgesic in some European countries), remain the

only KCNQ channel activators to receive approval for clinical use (Blackburn-Munro et al., 2005; Orhan et al., 2012). Retigabine has been used as an adjunct therapeutic in drug-resistant epilepsies, with additional interest and investigation into its effectiveness for treatment of tinnitus, pain, hypertension, and neurodegenerative disorders (Passmore et al., 2003; Li et al., 2013b; Wainger et al., 2014; Kalappa et al., 2015).

There is an abundance of literature describing preclinical investigation of retigabine in animal models of seizures but comparably little on the molecular mechanisms underlying its action on KCNQ channels (Gunthorpe et al., 2012; Large et al., 2012). Retigabine causes a dramatic hyperpolarizing shift of the voltage dependence of activation, leading to enhanced KCNQ channel activation around the typical neuronal resting membrane potential and thus reduction of cellular excitability (Wuttke et al., 2005; Lange et al., 2009; Zhou et al., 2013). Retigabine-sensitive KCNQ2–5 channels share a conserved Trp side chain in the pore-forming S5 helix, which is essential for retigabine actions, and even conservative mutations to other aromatic side chains abolish the retigabine-induced gating shift (Schenzer et al., 2005; Kim et al., 2015). In addition to this conserved Trp,

¹Department of Pharmacology, Alberta Diabetes Institute, University of Alberta, Edmonton, Alberta, Canada; ²Department of Drug Design and Pharmacology (Center for Biopharmaceuticals), University of Copenhagen, Copenhagen, Denmark.

Correspondence to Harley T. Kurata: kurata@ualberta.ca.

© 2018 Yau et al. This article is distributed under the terms of an Attribution–Noncommercial–Share Alike–No Mirror Sites license for the first six months after the publication date (see <http://www.rupress.org/terms/>). After six months it is available under a Creative Commons License (Attribution–Noncommercial–Share Alike 4.0 International license, as described at <https://creativecommons.org/licenses/by-nc-sa/4.0/>).

other side chains in the KCNQ pore have been shown to influence retigabine sensitivity but are not strictly required (Lange et al., 2009). A recent report from our group has suggested the chemical basis for retigabine interaction with this conserved Trp is a hydrogen bond formed between the drug and the indole N-H group (Kim et al., 2015). Retigabine interaction with the pore domain generates a shift in the voltage sensor equilibrium through a PIP₂-mediated coupling between the pore and voltage-sensing domain (Telezhkin et al., 2013; Soldovieri et al., 2016; Kim et al., 2017). Many complexities remain unresolved in our understanding of KCNQ activators. Most striking is the growing recognition of a variety of chemical scaffolds with KCNQ-activating properties and the likelihood that multiple mechanisms of action and binding sites may be targeted by this drug family (Padilla et al., 2009; Wang et al., 2017; Miceli et al., 2018).

Although channels formed by KCNQ2–5 subunits likely comprise four retigabine-binding sites, it has not been established how retigabine occupancy is translated to channel opening. We have addressed this question by investigating the functional stoichiometry of retigabine actions by manipulating the number of available retigabine-sensitive subunits in concatenated KCNQ3 channels. We demonstrate that in the presence of intermediate retigabine concentrations, channels exhibit biphasic conductance–voltage relationships. This behavior suggests that retigabine can exert its effects in a nearly “all-or-none” manner, with channels exhibiting either fully shifted or unshifted behavior. Using concatenated channels containing defined numbers of retigabine-sensitive subunits, we demonstrate that a single retigabine-sensitive subunit is required for a nearly maximal retigabine effect. As described in a companion paper (see Wang et al. in this issue), this property of retigabine contrasts with the voltage sensor-targeted KCNQ channel opener ICA-069673, which requires four drug-sensitive subunits to exert its full effect.

Materials and methods

Molecular biology and *Xenopus laevis* oocyte injections

Monomeric KCNQ3[A315T] channel cDNA was propagated and manipulated using the pSRC5 vector (gift of Dr. M. Tagliatela, University of Naples, Italy, and Dr. T. Jentsch, Max-Delbrück-Centrum für Molekulare Medizin, Germany). In all experiments involving homomeric expression of KCNQ3 channels, the Ala315Thr mutation was introduced to enable efficient trafficking of homomeric KCNQ3 (throughout the text, we refer to KCNQ3[Ala315Thr] as KCNQ3*; Zaika et al., 2008). Concatemeric constructs of KCNQ3* were generated by first creating dimers of combinations of KCNQ3* and KCNQ3*[W265F] and subcloning copies of the cDNA sequence into the NheI-XhoI or XhoI-EcoRV restriction sites of pcDNA3.1(–). PCR primer design omitted a stop codon from the leading subunit, while preserving a stop codon in the trailing subunit. Sequences of individual inserts were confirmed by Sanger sequencing before combining them by restriction digestion and ligation, leading to a dimer of the form: NheI-COPY1(no stop)-XhoI-COPY2-STOP-EcoRV. A second set of dimers was constructed with one subunit in the NheI-XhoI position (stop codon omitted) and a second subunit cloned in the XhoI-EcoRV position but with an engineered *NheI* site. These sec-

ond dimers had the form NheI-COPY1(no stop)-XhoI-COPY2(no stop)-NheI-EcoRV. Using an *NheI* digestion and ligation to combine these dimers, we generated a variety of tetrameric channel combinations of the form NheI-COPY1(no stop)-XhoI-COPY2(no stop)-NheI-COPY3(no stop)-XhoI-COPY4(STOP)-EcoRV, in pcDNA3.1(–). No linker sequences were added between any of the protomers. Sequences across the junctions were as follows (bold indicates the restriction site and additional amino acids introduced): junction 1 and 3 (NheI), 5'-AATAAGCCCATTCTCGAGGGGCTCAAGGCG-3' (amino acid sequence: NKPILEGLKA); junction 2 (XhoI), 5'-AATAAGCCCATTGCTAGCGGGCTCAAGGCG-3' (amino acid sequence: NKPIASGLKA).

Complementary RNA (cRNA) was transcribed from the cDNA using the mMessage mMachine kit (Ambion). Homomeric KCNQ3* constructs in pSRC5 were linearized with ApaI and transcribed using a T7 primer. Concatenated KCNQ3* constructs in pcDNA3.1(–) were linearized with BglII and transcribed using a T7 primer. Stage V–VI *X. laevis* oocytes were prepared as previously described and injected with cRNA. KCNQ3* in pSRC5 generates very large ionic currents within a day of injection. Tetrameric constructs in pcDNA3.1(–) were slower to express than monomeric KCNQ3* channels, usually requiring incubation times of ≥48 h at 18°C before recording.

Western blot and antibodies

Lysates from HEK cells transfected with KCNQ3* channel constructs were separated by gel electrophoresis on 0.7% SDS-PAGE gels and transferred to nitrocellulose blots using standard protocols. KCNQ3 protein was probed with a rabbit polyclonal antibody (APC-051; Alomone) and HRP-conjugated mouse anti-rabbit secondary antibody (ABM) and visualized using chemiluminescence (ECL Western blotting reagent; Pierce) and a FluorChem SP Gel Imager.

Two-electrode voltage clamp, solutions, and pharmacology

Voltage-clamped potassium currents were recorded in modified Ringer's solution (116 mM NaCl, 2 mM KCl, 1 mM MgCl₂, 0.5 mM CaCl₂, and 5 mM HEPES, pH 7.4) using an OC-725C voltage clamp (Warner). Glass microelectrodes were backfilled with 3 M KCl and had resistances of 0.1–1 MΩ. Data were filtered at 5 kHz and digitized at 10 kHz using a Digidata 1440A (Molecular Devices) controlled by pClamp 10 software (Molecular Devices). Retigabine was purchased from Toronto Research Chemicals, stored as a 100 mM stock in DMSO, and diluted to working concentrations each experimental day.

Patch-clamp recordings and fast solution exchange

For rapid solution exchange experiments with retigabine, we used transfected HEK 293 cells. HEK293 cells were maintained in DMEM supplemented with 10% FBS and 1% penicillin/streptomycin. Cells were grown in Falcon tissue culture-treated flasks, in an incubator at 5% CO₂ and 37°C. Cells were plated onto 12-well plates and allowed to settle for 24–48 h before transfection. Cells were transiently transfected with 1 μg of DNA encoding the channel of interest and 500 ng of GFP using jetPRIME DNA transfection reagent (Polyplus). 24 h after transfection, cells were plated onto sterile coverslips for electrophysiology experiments

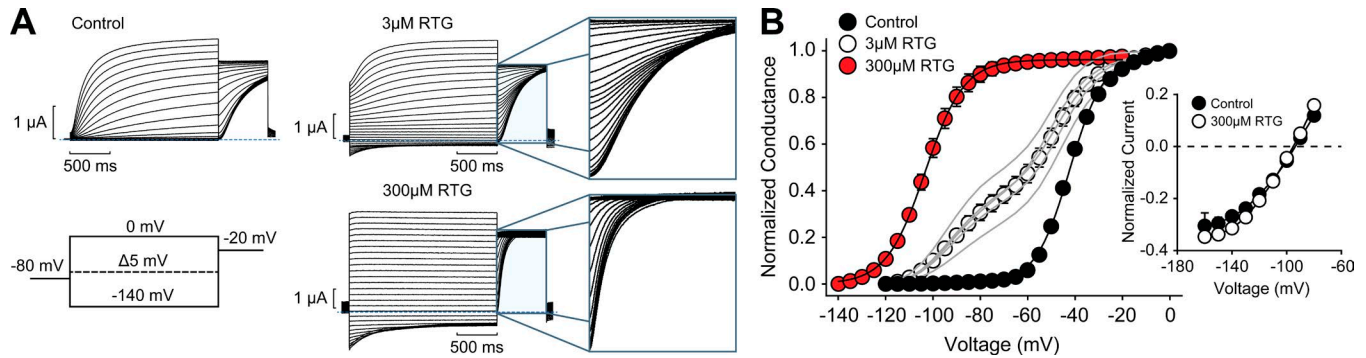


Figure 1. A biphasic conductance–voltage relationship emerges at intermediate retigabine concentrations. (A) Two-electrode voltage-clamp recordings from *X. laevis* oocytes expressing KCNQ3* after exposure to 0, 3, and 300 μM retigabine (RTG). Oocytes were held at -80 mV and depolarized for 2 s to voltages between -140 mV and $+20$ mV (in 5-mV steps), followed by repolarization to a -20 mV test potential. Highlighted in the insets are the tail currents elicited at -20 mV in 3 μM retigabine, illustrating the clustering of tail current amplitude at intermediate voltages and the saturating effect in 300 μM retigabine. **(B)** Conductance–voltage relationships were determined in different retigabine concentrations using normalized tail current amplitudes immediately after the voltage step to -20 mV. Gray lines are fits (sum of two Boltzmann equations) of data from individual oocytes in 3 μM retigabine, and the circles represent averages. Fully activated currents near the reversal potential were measured by stepping through a range of voltages after an activating prepulse to 20 mV (inset). Peak tail current magnitude was normalized to currents elicited at 20 mV. Retigabine does not appear to alter the reversal potential of KCNQ3-mediated currents.

the following day. Solutions were delivered at room temperature by pressure-driven flow through a multibarreled solution delivery turret driven by the RSC-200 (Biological) rapid solution exchanger to enable solution jumps.

Whole-cell patch-clamp recordings were performed using extracellular solution consisting of 135 mM NaCl, 5 mM KCl, 2.8 mM Na acetate, 1 mM $\text{CaCl}_2(2\text{H}_2\text{O})$, 1 mM $\text{MgCl}_2(6\text{H}_2\text{O})$, and 10 mM HEPES, with pH adjusted to 7.4. Intracellular solution contained 135 mM KCl, 5 mM EGTA, and 10 mM HEPES, with pH adjusted to 7.3. Glass pipette tips were manufactured using soda lime glass (Fisher Scientific) and had tip resistances of 1–3 $\text{M}\Omega$ in standard experimental solutions. Series resistance compensation of 75–85% was used in all recordings, and uncompensated series resistance did not exceed 4 $\text{M}\Omega$. Recordings were filtered at 5 kHz and sampled at 10 kHz using an Axopatch-200B Digidata 1440A controlled by pClamp 10 software.

Data analysis

Voltage dependence of channel activation was fitted with a two-component Boltzmann equation of the form $G/G_{\text{max}} = a / (1 + e^{-(V - V_{1/2,a})/k_a}) + (1 - a) / (1 + e^{-(V - V_{1/2,b})/k_b})$, where $V_{1/2,a}$ and $V_{1/2,b}$ are the voltages, where each component is half-maximal, and k_a and k_b are slope factors reflecting the voltage range over which an e-fold change in open probability (P_o) of the respective component is observed. In saturating drug conditions, or in control conditions, only a single component was required for an adequate fit. Concentration responses were fit with the following equation: Normalized conductance = $G_{(0 \text{ RTG})} + (1 - G_{(0 \text{ RTG})}) / (1 + (\text{EC}_{50}/[\text{RTG}])^n)$, where $G_{(0 \text{ RTG})}$ is the conductance in zero retigabine, EC_{50} is the retigabine concentration that causes a half-maximal increase of normalized conductance, and n is a Hill coefficient.

Online supplemental material

Fig. S1 replots data from Fig. 5 to illustrate different responses to intermediate retigabine concentrations the concatenated channel constructs. Fig. S1 also provides conductance–voltage

relationships collected from individual oocytes injected with the WFFF tetramer.

Results

KCNQ3 as a model to investigate retigabine stoichiometry

KCNQ2–5 channels exhibit a pronounced hyperpolarizing shift of the voltage dependence of activation in the presence of saturating concentrations of retigabine. In addition to the pore domain-delimited binding site for retigabine, other reports have suggested an alternative binding site for certain KCNQ openers, such as ICA-069673, in the voltage-sensing domain (Padilla et al., 2009; Gao et al., 2010; Li et al., 2013a; Wang et al., 2017, 2018). This alternative site has prominent effects in KCNQ2, but is absent or only weakly effective in KCNQ3 channels. Thus, homomeric KCNQ3 is a good model to selectively investigate retigabine interactions and effects via the conserved pore site. Although reports vary slightly in terms of the magnitude of the retigabine-mediated gating shift, we routinely observe large shifts of ~ 60 mV (Fig. 1, A and B) in saturating concentrations of retigabine (100–300 μM) for KCNQ3* channels (shorthand used throughout to refer to homomeric KCNQ3[A315T], see Materials and methods) expressed in *X. laevis* oocytes (Kim et al., 2015).

Biphasic conductance–voltage relationships at intermediate retigabine concentrations

In experiments measuring retigabine effects on KCNQ3*, we previously observed a shallow slope of the conductance–voltage relationship at intermediate retigabine concentrations when compared with control or saturating conditions (Kim et al., 2015). We investigated this phenomenon in more detail with closely spaced voltage steps and observed prominent “splitting” of the conductance–voltage relationship into two components. This is apparent in Fig. 1 A (3 μM retigabine), in which tail current magnitudes are closely spaced after prepulses to intermediate voltages, leading to a shallow slope (plateau) between -80 mV and -50 mV in the conductance–voltage relationship (Fig. 1 B).

Table 1. Double Boltzmann fit parameters for KCNQ3* activation in a range of retigabine concentrations

RTG concentration (μM)	Shifted component, a	$V_{1/2a}$ (mV)	$V_{1/2b}$ (mV)	k_a	k_b	n
0	—	—	-41.8 ± 0.7	—	7.6 ± 0.2	5
1	0.12	-93.3 ± 0.7	-46.0 ± 1.1	5.9 ± 0.4	9.2 ± 0.3	5
3	0.32	-93.5 ± 0.3	-48.3 ± 1.2	6.9 ± 0.1	9.9 ± 0.6	5
10	0.72	-98.8 ± 0.7	-62.0 ± 1.7	7.6 ± 0.2	11.4 ± 0.5	5
30	1	-97.4 ± 2.4	—	9.4 ± 1.3	—	5
100	1	-103.3 ± 0.8	—	7.9 ± 0.7	—	5
300	1	-102.0 ± 1.5	—	9.2 ± 0.8	—	5

Conductance–voltage relationships were fit with the equation $G/G_{\text{max}} = a/(1 + e^{-(V-V_{1/2,a})/k_a}) + (1 - a)/(1 + e^{-(V-V_{1/2,b})/k_b})$. Data presented are mean \pm SEM.

The retigabine-mediated shift in voltage dependence does not significantly alter the reversal potential (Fig. 1 B, inset). The biphasic conductance–voltage relationship is well fit with a sum of two Boltzmann functions (Table 1). There is a dose-dependent increase in the contribution of the shifted component of the conductance–voltage relationship, with the retigabine-shifted component becoming more prominent with increasing retigabine concentrations (Fig. 2 A). Using the magnitude of the shifted fraction, we calculated an EC_{50} of $4.4 \mu\text{M}$ with a Hill coefficient close to 1 (Fig. 2 B). There is a modest increase of the $V_{1/2}$ of the shifted component from -93.3 ± 0.3 mV at $1 \mu\text{M}$ retigabine to -103.3 ± 0.8 mV at saturating concentrations (Table 1). In addition, the “unshifted” component was best fit with a $V_{1/2}$ of -41.8 ± 0.7 mV in control conditions and progressed to more hyperpolarized $V_{1/2}$ values at higher retigabine concentrations. At the highest retigabine concentrations, we could not confidently generate fit parameters for the unshifted component, and so we only reported parameters for a single-component Boltzmann fit. We also generated concentration–response curves using the normalized conductance at -60 mV (a voltage where retigabine actions are prominent), yielding similar fit parameters (Fig. 2 C).

Generation of a concatenated KCNQ3* construct

The retigabine-induced biphasic conductance–voltage relationships suggest the possibility that retigabine acts roughly in an all-or-none manner, reminiscent of recently reported effects of γ -subunits of BK (KCNMA1) channels (Gonzalez-Perez et al., 2014, 2015). Although a variety of mechanisms might underlie a biphasic conductance at a given drug concentration, our observation that increased retigabine concentrations cause an increased magnitude of the shifted component suggests that most channels are distributed between an unshifted state and a fully shifted state. To a rough approximation, altered drug concentrations appear to govern the ratio of channels in shifted and unshifted modes, as opposed to a progressive concentration-dependent shift of the $V_{1/2}$ to more hyperpolarized voltages.

As described for BK channel modulation by γ -subunits, numerous stoichiometric channel/modulator configurations can generate an apparent all-or-none effect (Gonzalez-Perez et al., 2014). Experiments with homomeric KCNQ3* do not definitively demonstrate the number of retigabine molecules required to induce the shifted gating mode in KCNQ3* and do not demon-

strate whether varying numbers of retigabine-sensitive subunits within a channel generate differential gating shifts. To investigate the stoichiometry of retigabine effects, we generated concatenated KCNQ3 channel constructs with varying numbers of KCNQ3* versus Trp265Phe subunits (Schenzer et al., 2005; Wuttke et al., 2005). Throughout the study, W refers to a WT Trp265-containing subunit, and F refers to a Trp265Phe mutant subunit (e.g., WWFF contains two WT subunits, and two Trp265Phe subunits). We confirmed that our plasmids encoded expression of full-length tetramers using Western blots (Fig. 3 A) and also confirmed that concatenated channels exhibited similar gating properties relative to homomeric KCNQ3* channels (Fig. 3, B and C). We had difficulties using the KCNQ3 antibody on lysates from *X. laevis* oocytes because of a high background signal, so Western blots were generated from lysates from HEK293 cells transfected with the same pcDNA3.1(–) concatenated channel constructs that were used to generate mRNA for oocyte recordings (Fig. 3 A). At high concentrations of loaded protein (leftmost well, Fig. 3 A), KCNQ3* (monomeric) channels exhibited a weak signal at a high molecular weight that likely reflects some oligomerization (left lane), although it primarily migrated as a monomer. At lower KCNQ3* concentrations (right lane), this higher-molecular-weight band was not as prominent. The higher-molecular-weight band did not perfectly align with the KCNQ3 signal from concatenated channels. Previous studies of concatenated tetrameric KCNQ1 (Meisel et al., 2012) and KCNQ2 (Gourgy-Hacohen et al., 2014) also compared monomeric and tetrameric constructs using Western blots, although their concatenation strategy was different from ours. Overall, it is challenging to definitively demonstrate whether the higher order oligomers align perfectly with the concatemers. However, our findings and these studies demonstrate that concatemeric constructs generate high molecular weight translated protein, suggesting that premature termination of translation (or spurious initiation of translation within the channel sequence) is infrequent. In our case, we were also reassured that all concatemers ran at a similar molecular weight, confirming that construction of the concatenated channel plasmids was consistent. We also validated the basic function of all the concatemers by demonstrating similar gating kinetics and voltage dependence as KCNQ3* in control conditions (Fig. 3, B and C). Similar to previous reports in KCNQ1 and KCNQ2, the voltage-dependent gating properties of

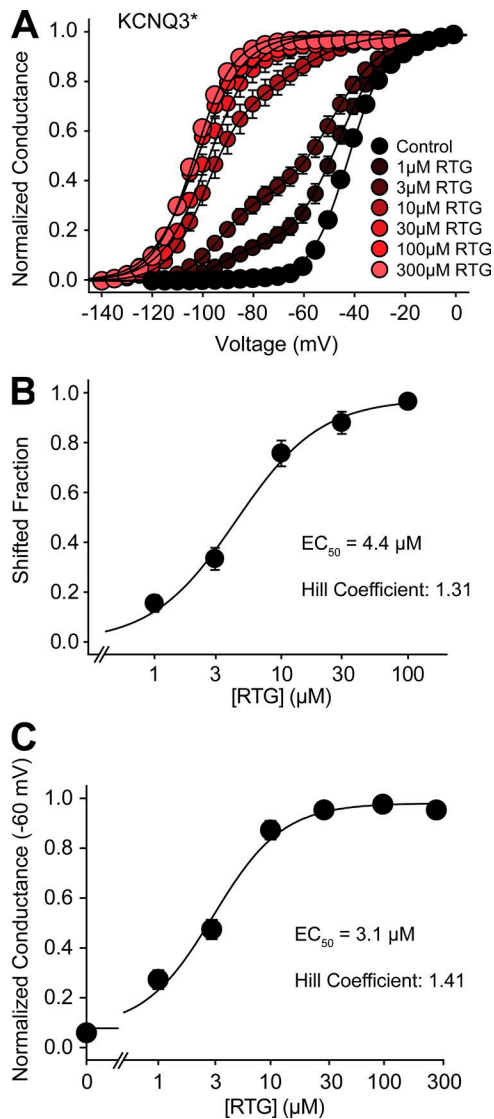


Figure 2. Conductance–voltage relationships for KCNQ3* in different retigabine concentrations. (A) Conductance–voltage relationships were determined over a range of retigabine (RTG) concentrations using normalized tail current amplitudes from the same voltage step protocol as Fig. 1 A. Conductance–voltage relationships are fit with the sum of two Boltzmann equations (fit parameters are summarized in Table 1). (B and C) The concentration response to retigabine was determined using the fraction of the shifted Boltzmann component (B) or the normalized current (–60 mV; C) at different retigabine concentrations and fit with a Hill equation. Data presented are mean \pm SEM.

the KCNQ3* concatemers closely resembled homomeric KCNQ3* channels (Meisel et al., 2012; Gourgy-Hacohen et al., 2014).

A single retigabine-sensitive subunit results in a large retigabine effect

We further validated the tetrameric construct design by directly comparing the retigabine sensitivity of the WWWW tetramer with homomeric KCNQ3* channels. Fit data over a range of retigabine concentrations (KCNQ3* from Fig. 2) is overlaid on WWWW data in Fig. 4 A for direct comparison. Conductance–voltage relationships exhibited similar biphasic properties in re-

sponse to retigabine. The properties of currents generated from the WWWW tetramer are also similar to homomeric KCNQ3* channels, illustrated by exemplar traces in 3 μM retigabine that closely resemble our initial observations presented in Fig. 1 A. In addition, the concentration response of the tetrameric channel was very similar to KCNQ3* homomeric channels (Fig. 5).

We also characterized the retigabine response of concatenated channels with increasing numbers of retigabine-sensitive subunits (Fig. 5, A–D). All tetramers remained very responsive to retigabine although small differences were apparent at intermediate concentrations. For example, the WFFF tetramer (one retigabine-sensitive subunit) consistently exhibited a slightly smaller response relative to the other channels. These differences may be more apparent by examining conductance–voltage curves for each concatemer at a single retigabine concentration (see Fig. S1, A and B). In terms of the maximal retigabine response (maximum $\Delta V_{1/2}$), channels with one sensitive subunit (WFFF) exhibited a shifted $V_{1/2}$ of -91.9 ± 0.7 mV, slightly smaller than the WWWW tetramer ($V_{1/2} = -103 \pm 3$ mV). Channels with intermediate numbers of retigabine-sensitive subunits exhibited intermediate effects, but it is apparent that much of the maximal retigabine effect can be accounted for by a single drug-sensitive subunit (see maximally shifted conductance–voltage relationships in Fig. 5 F).

We compared retigabine sensitivity using the normalized conductance at –60 mV (Fig. 5 E). The apparent affinity increased slightly in channels with greater numbers of retigabine-sensitive subunits (Fig. 5 E), but the affinity did not vary as steeply with subunit composition as one would predict with a simple model of four independent binding sites (WWWW $EC_{50} = 4 \mu\text{M}$; WFFF $EC_{50} = 7.7 \mu\text{M}$). This observation may imply a cooperative response to retigabine binding, although this will require further study and validation given some of the challenges associated with these experiments. For example, we have observed that retigabine effects on KCNQ3 channels expressed in *X. laevis* oocytes become larger with longer incubation in the presence of the drug, and although we have maintained exposure times constant, this is certainly a likely source of uncertainty and variability. We also noted we may have failed to detect the full gating shift of the WFFF and WWWW concatemers (this is hinted by the shallower slope factor k for WFFF and WFFF in saturating retigabine; Table 2), but it is not practical to apply higher concentrations of retigabine, because drug solubility becomes an issue. It is also noteworthy that all of the concatenated channels, including the “single-site” WFFF, could reproduce the biphasic conductance–voltage relationships observed in KCNQ3* homomeric channels or the WWWW tetramer. Although the effect in WFFF does not appear to be quite as pronounced as WWWW in the averaged data, examination of records from individual oocytes illustrates the biphasic conductance–voltage relationship more clearly (Fig. S1 C). These observations suggest that a single functional retigabine site is sufficient to nearly completely shift the voltage dependence of channel gating. It was also interesting that the maximally shifted $V_{1/2}$ measured in the WFFF tetramer ($V_{1/2} = -91.9 \pm 0.7$ mV) is similar to the shifted $V_{1/2}$ component measured at low retigabine concentrations (e.g., 3 μM) in either KCNQ3* channels ($V_{1/2} = -93.5 \pm 0.5$ mV; Fig. 2 A), or WWWW tetramers ($V_{1/2} = -93 \pm 2$

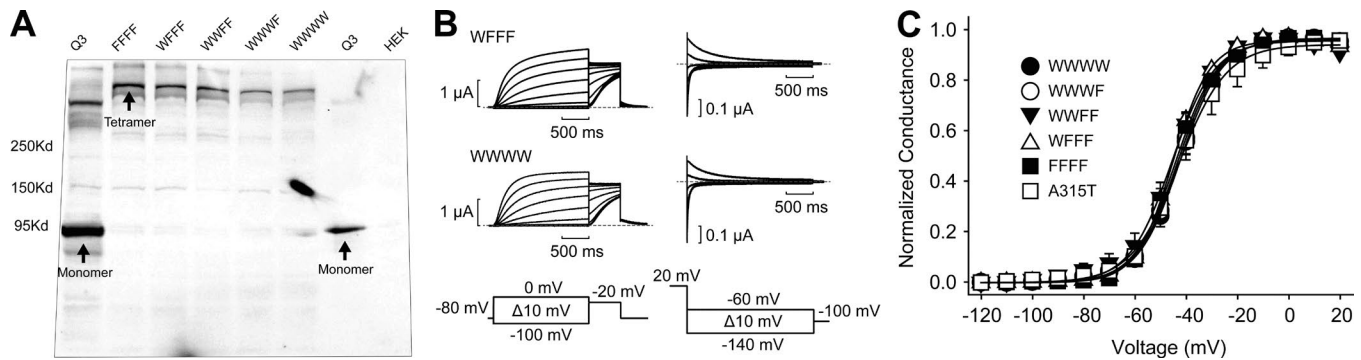


Figure 3. **Generation of KCNQ3* concatemers with variable stoichiometry of retigabine-sensitive subunits.** (A) Western blots obtained from HEK293 cells expressing tetrameric constructs show predominant expression of tetrameric KCNQ3 protein, and the absence of monomeric subunits, in comparison to cells transfected with monomeric KCNQ3* control. (B and C) Representative activation and deactivation kinetics and summarized conductance–voltage relationships for all concatenated KCNQ3* channel constructs (W represents a native Trp at position 265, and F represents a Trp265Phe mutant subunits). No significant differences in $V_{1/2}$ or slope factor were detected in comparisons between the different concatenated channel types. Data points are mean \pm SEM.

mV; Fig. 4 A). Although perhaps coincidental, this similar effect may suggest that the shifted component observed in low retigabine concentrations corresponds to a fraction of channels that are predominantly bound to a single retigabine molecule.

The retigabine-induced gating shift involves changes to both the activation (accelerated) and deactivation (decelerated) kinetics of KCNQ3*. We compared the saturating effects of retigabine on channel gating kinetics in the series of KCNQ3* tetrameric channel constructs over a range of voltages (Fig. 6). Overall, activation kinetics are accelerated similarly whether channels have a full complement of four retigabine-sensitive subunits or just a single subunit (Fig. 6 B). Also, deactivation kinetics is decelerated by retigabine by a comparable extent whether there are one or four retigabine-sensitive subunits present (Fig. 6 C). These findings are consistent with the effects observed on the conductance–voltage relationship, suggesting that a single retigabine-sensitive subunit can account for most of the maximal retigabine effect.

Retigabine simultaneously occupies multiple drug-sensitive subunits

Although our findings demonstrate that a single drug-sensitive subunit can account for most of the effects of retigabine, these

experiments do not distinguish whether multiple drug-sensitive subunits can be occupied simultaneously by retigabine. We directly tested this possibility using rapid solution exchange with HEK293 cells expressing either the WWWW or WFFF tetramers (Fig. 7). We held channels at various voltages after exposure to retigabine and then rapidly washed off the drug (exemplar sweeps at -20 mV and -60 mV are shown in Fig. 7). In the WFFF tetramer, retigabine wash off generates a monotonic reduction in current as the drug unbinds that is typically well described with a single time constant. This decay reflects a shift in the voltage dependence of activation as retigabine dissociates from the channels. In contrast, the WWWW tetramers exhibit a much more prominent delay of channel closure, leading to a clear sigmoidal reduction of current after rapid drug wash off (Fig. 7). This likely reflects dissociation of multiple drug molecules from the channel (while occupancy of a single subunit is sufficient to generate most of the shift in voltage-dependent gating), leading to a delayed current decay when multiple drug-sensitive subunits are present. Current decay in WWWW and WFFF tetramers was fit with a Hodgkin–Huxley-type equation of the form $I(t) = I_{(t=\infty)} + (I_{(t=0)} - I_{(t=\infty)}) \cdot (e^{-t/\tau})^n$, where $t = 0$ refers to the current immediately after retigabine wash off and $t = \infty$ refers to the steady-

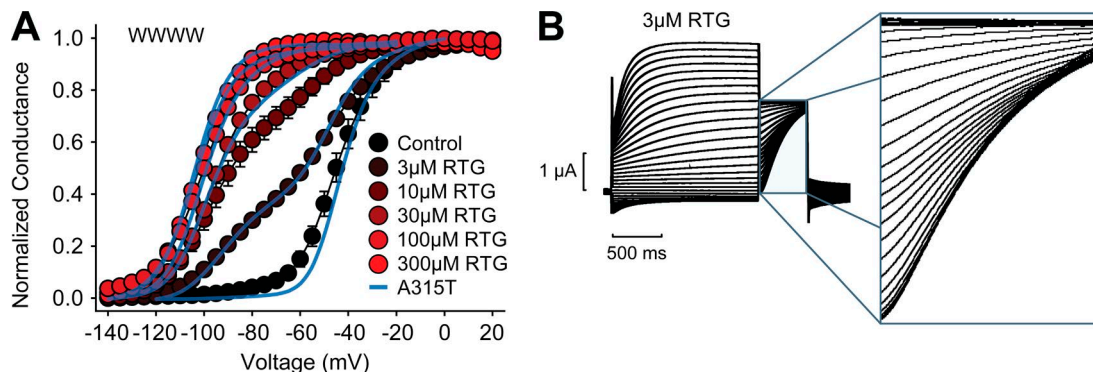


Figure 4. **WWWW concatenated channels exhibit similar retigabine responses as homomeric KCNQ3*.** (A) Conductance–voltage relationships were collected in multiple retigabine (RTG) concentrations using the same voltage protocol as Fig. 1. Overlaid blue curves are fits described in Fig. 2 and Table 1 for KCNQ3[A315T] channels (sum of two Boltzmann equations). Data are mean \pm SEM. (B) Exemplar currents collected in $3 \mu\text{M}$ retigabine, illustrating the progression of tail currents that underlie the biphasic conductance–voltage relationship.

Table 2. Fit parameters for activation of concatenated channels used in the study in control conditions and at saturating retigabine concentrations

Construct	Control $V_{1/2}$ (mV)	Max shifted $V_{1/2}$ (mV)	Control k (mV)	Max shifted k (mV)	n
WWWW	-44 ± 3	-103 ± 3	9.4 ± 1.1	7.8 ± 0.4	5
WWWF	-43.8 ± 0.7	-101.0 ± 1.3	6.9 ± 0.1	9.2 ± 0.1	5
WWFF	-44.1 ± 0.7	-93 ± 1	6.9 ± 0.1	12.0 ± 0.6	5
WFFF	-43.4 ± 1.2	-91.9 ± 0.7	9.3 ± 0.5	11.1 ± 0.2	5
FFFF	-42.8 ± 0.9	-46.3 ± 1	8.4 ± 0.9	7.3 ± 0.7	5

Conductance–voltage relationships were fit with the equation $G/G_{\max} = 1 / (1 + e^{-(V-V_{1/2})/k})$. Data are mean \pm SEM.

state current achieved after retigabine wash off. Current decay in WFFF tetramers was well fit with $n = 1$ or 2 ($\tau = 4,400 \pm 500$ ms at -20 mV and $4,600 \pm 500$ ms at -60 mV, $n = 6$). In contrast, current decay in WWWW tetramers was best fit with $n = 4$ ($\tau = 4,800 \pm 200$ ms at -20 mV and $4,600 \pm 200$ ms at -60 mV, $n = 5$). These findings support a general model that multiple subunits can bind to retigabine simultaneously, but drugs must unbind from all subunits to reverse the channel-activation effect.

Mutations of other side chains in the putative retigabine-binding site cause a gating “supershift” with pronounced biphasic features

Previous reports identified multiple amino acids in KCNQ2 or KCNQ3 channels that contribute to the putative retigabine-bind-

ing pocket in the pore domain (Fig. 8 A). Mutations in this region, such as KCNQ3, L314, or L272, weaken retigabine sensitivity, but unlike Trp 265, they are not absolutely required for drug effects (Lange et al., 2009; Kim et al., 2015). With the recognition of the unique effects of retigabine on the KCNQ3* conductance–voltage relationship, we also examined the retigabine sensitivity of these binding pocket mutations in more detail. As previously reported, some of these mutations (L314A, L272I) cause a modest depolarizing shift of channel activation relative to KCNQ3* in control conditions but retain a similar $V_{1/2}$ in saturating retigabine concentrations. Thus the maximal retigabine-mediated gating shift in these mutants is even larger than in WT KCNQ3*, and the biphasic nature of the conductance–voltage relationship is more pronounced (Fig. 8, C and D). Retigabine effects on these putative binding site mutants exhibits a similar progression of the magnitude of shifted and unshifted components, although higher retigabine concentrations are required than for KCNQ3* channels, reflecting the weaker retigabine sensitivity of these mutant channels (Fig. 8 B). This exaggerated biphasic nature of the conductance–voltage relationship (i.e., the absence of multiple intermediate components) adds confidence to our finding that intermediate retigabine concentrations cause channels to distribute primarily between nonshifted and fully shifted modes.

Discussion

Retigabine interaction with KCNQ2–5 potassium channels significantly alters the voltage dependence of channel activation (Schenzer et al., 2005; Wuttke et al., 2005). In the presence of saturating concentrations of retigabine, the hyperpolarizing shift of voltage dependence of these channels causes a greater

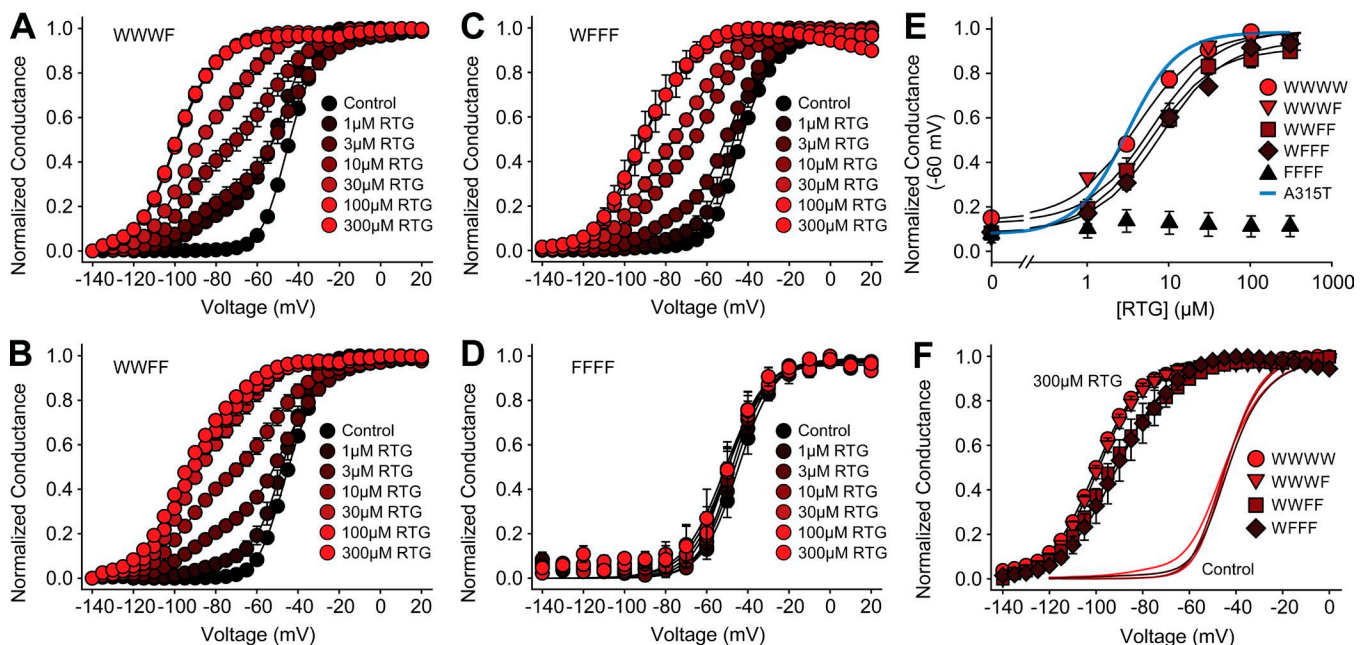


Figure 5. A single retigabine-sensitive subunit encodes a large retigabine effect. (A–D) Summary conductance–voltage relationships from WWWW (A), WWWF (B), WFFF (C), and FFFF (D) concatenated constructs, expressed in *X. laevis* oocytes and incubated in various retigabine (RTG) concentrations. **(E)** Summary data of the concentration–response of retigabine-mediated channel activation at -60 mV. **(F)** Maximal RTG-induced shift in $V_{1/2}$ for different constructs. See also Table 2 (data for FFFF are not shown). Data are mean \pm SEM.

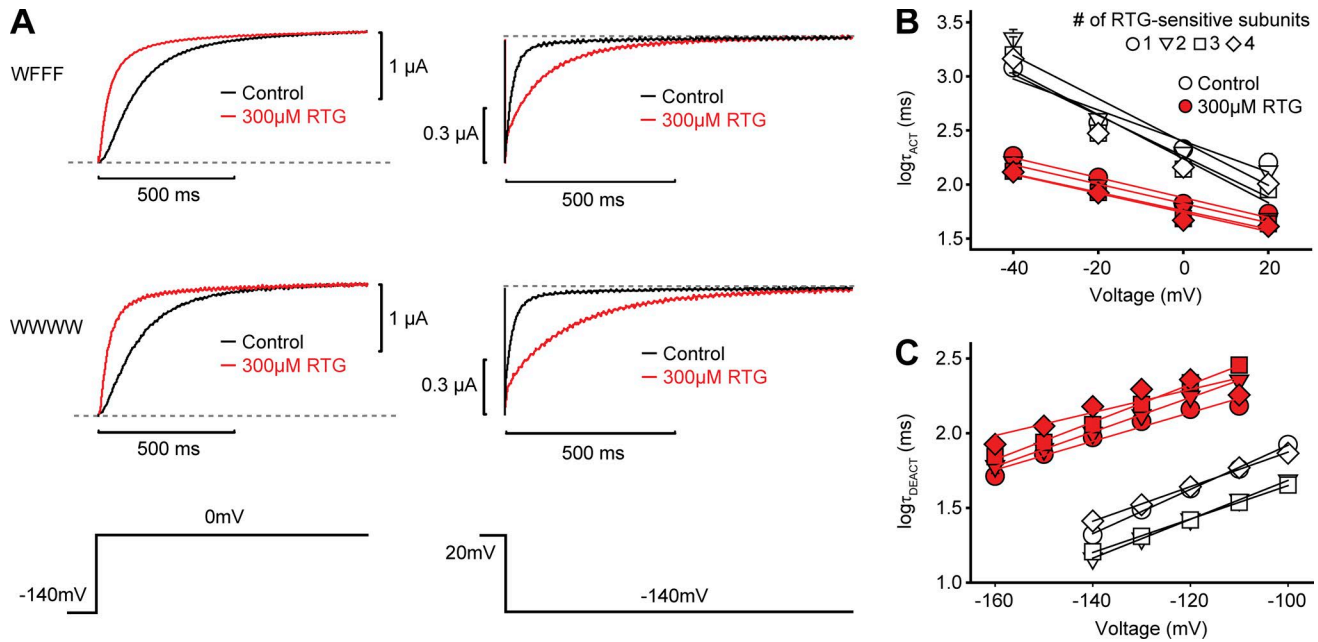


Figure 6. **Effects of retigabine on the activation and deactivation kinetics of KCNQ3* tetramers.** (A) Sample activation (left, 0-mV pulse) and deactivation (right, -140-mV pulse) traces obtained in the presence (red) or absence (black) of a saturating concentration of retigabine (RTG). (B and C) Summary of kinetic data for all concatenated KCNQ3* constructs ($\log\tau_{ACT}$, $\log\tau_{DEACT}$). Notice that kinetic effects of retigabine are apparent even in concatenated channels with a single retigabine-sensitive subunit. Data are mean \pm SEM.

fraction to remain open in the normal range of neuronal resting membrane potentials. This hyperpolarizing effect is thought to underlie the therapeutic benefit of retigabine in diseases of membrane excitability like epilepsy. Using homomeric KCNQ3*

channels as a model system, we investigated the number of retigabine-sensitive subunits required for a maximal retigabine response. We generated concatenated tetrameric subunits and varied the number of channel subunits carrying the Trp265Phe mutation previously shown to abolish retigabine sensitivity (Schenzer et al., 2005; Wuttke et al., 2005). It should be noted that KCNQ3*[Trp265Phe] mutant channels exhibit no response to the highest experimentally achievable concentrations of retigabine and are presumed to abolish binding, although no direct investigation of retigabine binding to WT or mutant channels has been reported (Kim et al., 2015). Because of this uncertainty, we have chosen to refer to the number of retigabine-sensitive subunits rather than the number of retigabine-binding sites.

The presence of a single retigabine-sensitive subunit was sufficient to reproduce most of the maximal retigabine response observed in homomeric KCNQ3* channels (Figs. 4 and 5). The kinetic effects of retigabine (acceleration of channel activation, deceleration of channel closure) were also consistent between the WFFF and WWWW concatenated channels. Collectively, these data suggest that a single retigabine-sensitive subunit is sufficient to generate nearly the full retigabine gating effect. This requirement for drug binding to a single subunit was also reflected in the kinetics of current decay observed after rapid wash off of retigabine. The presence of multiple drug-sensitive subunits results in a clear delay and sigmoidal time course of current decay, contrasting the monoexponential decay observed in WFFF tetramers. A consistent explanation for this observation is that the delay reflects unbinding of multiple retigabine molecules, as loss of channel potentiation would not be expected until the drug has unbound from all of the sensitive subunits. Monoexponential decay of the WFFF currents would then reflect reti-

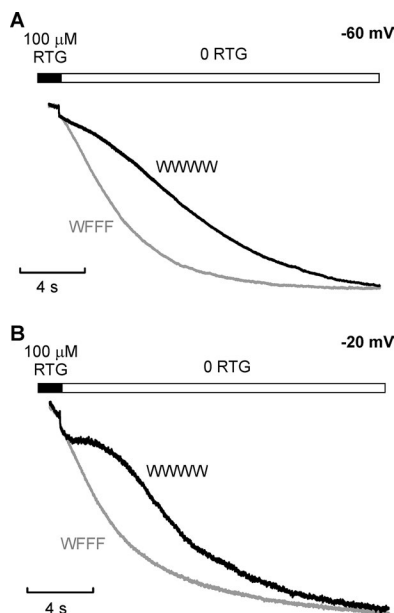


Figure 7. **Distinct current relaxation in WWWW and WFFF after rapid retigabine wash off.** (A and B) WWWW and WFFF concatemers were expressed in HEK293 cells, and currents were measured by patch clamp. Cells were held at various voltages, and a rapid solution-switching system was used to apply retigabine, followed by a rapid wash off into control conditions. Exemplar traces illustrating current relaxation after retigabine wash off are presented for WWWW and WFFF at -60 mV (A) and -20 mV (B), as indicated.

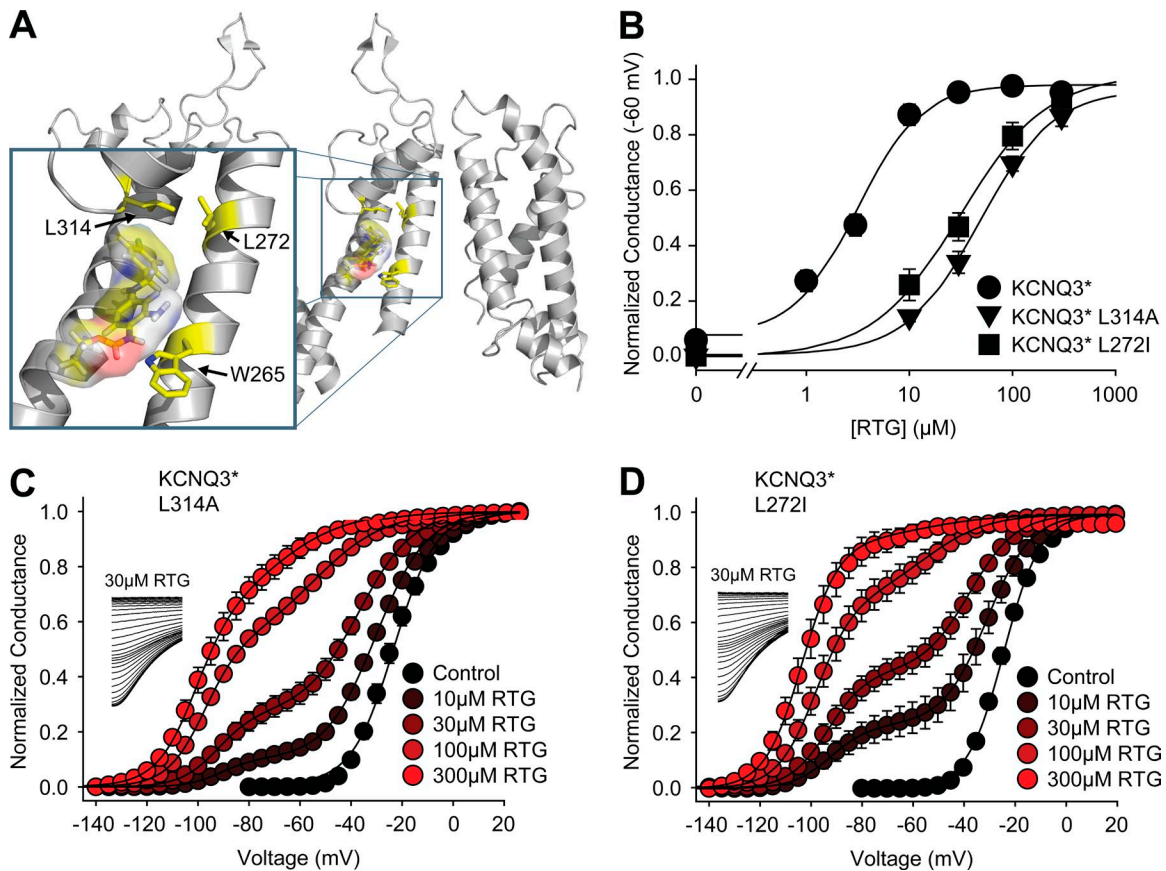


Figure 8. **Supershifted retigabine-binding site mutants highlight an all-or-none shift.** (A) Molecular model highlighting the positioning of L314 and L272 in close proximity to W265 in the putative retigabine (RTG)-binding site (residues highlighted in yellow). (B) Concentration responses of KCNQ3* and binding site mutants measured using the normalized conductance at -60 mV. (C and D) Summary conductance-voltage relationships obtained from KCNQ3*[L314A] and KCNQ3*[L272I] channels in different retigabine concentrations using the same protocol as Figure 1. Inset panels display sample tail current recordings in 30 μ M retigabine, clearly highlighting clustered tail currents after prepulses to intermediate voltages.

gabine unbinding from a single site (Fig. 7). Importantly, there are sometimes shortcomings or inconsistencies that arise when using a concatenation strategy that have been suggested to arise from unexpected assembly of subunits from different concatemers (McCormack et al., 1992; Sack et al., 2008). We have not been able to explicitly rule out assembly of higher-order oligomers of concatenated constructs in our study, but the observed differences in the retigabine sensitivity of different concatemers (Fig. 5), and particularly the kinetics of retigabine dissociation (Fig. 7), suggest the concatemers assemble as predicted.

An exaggerated biphasic response to retigabine could be engineered in supershifted channels carrying binding site mutations (Fig. 8). This observation is important, as it renders the biphasic nature of the conductance-voltage response much clearer (as opposed to a mixture of three or four Boltzmann components that might be less apparent in the data for homomeric KCNQ3* channels in Fig. 1). Interestingly, retigabine appears able to fully overcome the destabilization of channel opening caused by these binding site mutations rather than making a constant energetic contribution to intrinsic open state stability of the mutant channel. This may be important in disease-causing loss-of-function KCNQ2 or KCNQ3 mutations linked to epilepsies and whether retigabine might be an effective therapeutic in some of these cases.

Second, the biphasic nature of voltage sensitivity in the presence of retigabine may influence how one considers dosing effects of the drug in clinical conditions. A drug causing a progressive hyperpolarizing shift of channel activation while maintaining a steep voltage sensitivity might be expected to have a steep concentration dependence over which the drug becomes effective at a given voltage. In contrast, a gradual shift in the fraction of shifted/"potentiated" channels at a given voltage might broaden the range over which the drug can have a biological effect. Although a retigabine-induced biphasic conductance-voltage relationship has not been previously reported for KCNQ2/3 channels, it has probably not been examined in detail and may be difficult to resolve, because (for reasons that remain unclear) KCNQ2/3 heteromers exhibit a smaller retigabine-induced $\Delta V_{1/2}$ than KCNQ2 or KCNQ3* homomeric channels (Kim et al., 2015).

Lastly, it is important to consider the mechanism underlying the biphasic nature of the conductance-voltage relationship in the presence of retigabine. In the case of γ -subunit regulation of BK channels, random assembly of BK channels with different numbers of auxiliary subunits is presumed to govern the division of channels into populations with distinct gating properties (Gonzalez-Perez et al., 2015). However, in the case of a small molecule, one might expect channel-drug interactions to be more

transient or dynamic. In this particular experiment, the biphasic nature of the conductance–voltage relationship likely reflects the affinity of retigabine binding to closed/resting channel states during the interpulse interval. At low concentrations, only a fraction of channels will be bound to retigabine during the interpulse interval and will be able to open at relatively negative voltages. To clearly divide available channels into distinct populations, we presume that slow binding and unbinding kinetics of retigabine (relative to the time scale of the experimental voltage pulses) are important to generate this feature in the data.

In conclusion, this study demonstrates that interaction of the prototype pore-targeted KCNQ channel opener retigabine with a single retigabine-sensitive subunit is sufficient to generate a nearly maximal drug-induced gating shift. In a companion paper (Wang et al., 2018), this finding is compared with an alter class of KCNQ channel openers that appear to target a distinct site in the voltage sensor and require a full complement of four drug-sensitive subunits to generate a maximal drug effect.

Acknowledgments

This study was funded by Canadian Institutes of Health Research operating grant MOP 142482. C.K. Wang was supported by a Canadian Institutes of Health Research CGS-M graduate award. R.Y. Kim was supported by a Canadian Institutes of Health Research CGS-D graduate award. H.T. Kurata is supported by a Canadian Institutes of Health Research New Investigator Award and the Alberta Diabetes Institute. S.A. Pless was supported by a Lundbeck Foundation Fellowship (R139-2012-12390).

M. Yau, S. Pless, and H. Kurata designed the experiments. M. Yau, R. Kim, C. Wang, J. Li, T. Ammar, and R. Yang performed experiments and analyzed data. M. Yau, S. Pless, and H. Kurata wrote the manuscript. All authors provided edits and approved the final version of the manuscript.

The authors declare no competing financial interests.

Author contributions: M. Yau, S. Pless, and H. Kurata designed the experiments. M. Yau, R. Kim, C. Wang, J. Li, T. Ammar, and R. Yang performed experiments and analyzed data. M. Yau, S. Pless, and H. Kurata wrote the manuscript. All authors provided edits and approved the final version of the manuscript.

Kenton J. Swartz served as editor.

Submitted: 26 January 2018

Accepted: 6 August 2018

References

- Bentzen, B.H., N. Schmitt, K. Calloe, W. Dalby Brown, M. Grunnet, and S.P. Olesen. 2006. The acrylamide (S)-1 differentially affects Kv7 (KCNQ) potassium channels. *Neuropharmacology*. 51:1068–1077. <https://doi.org/10.1016/j.neuropharm.2006.07.001>
- Biervert, C., B.C. Schroeder, C. Kubisch, S.F. Berkovic, P. Propping, T.J. Jentsch, and O.K. Steinlein. 1998. A potassium channel mutation in neonatal human epilepsy. *Science*. 279:403–406. <https://doi.org/10.1126/science.279.5349.403>
- Blackburn-Munro, G., W. Dalby-Brown, N.R. Mirza, J.D. Mikkelsen, and R.E. Blackburn-Munro. 2005. Retigabine: chemical synthesis to clinical application. *CNS Drug Rev.* 11:1–20. <https://doi.org/10.1111/j.1527-3458.2005.tb00033.x>
- Brown, D.A., and P.R. Adams. 1980. Muscarinic suppression of a novel voltage-sensitive K⁺ current in a vertebrate neurone. *Nature*. 283:673–676. <https://doi.org/10.1038/283673a0>
- Brown, D.A., and G.M. Passmore. 2009. Neural KCNQ (Kv7) channels. *Br. J. Pharmacol.* 156:1185–1195. <https://doi.org/10.1111/j.1476-5381.2009.00111.x>
- Brown, D.A., S.A. Hughes, S.J. Marsh, and A. Tinker. 2007. Regulation of M(Kv7.2/7.3) channels in neurons by PIP(2) and products of PIP(2) hydrolysis: significance for receptor-mediated inhibition. *J. Physiol.* 582:917–925. <https://doi.org/10.1113/jphysiol.2007.132498>
- Charlier, C., N.A. Singh, S.G. Ryan, T.B. Lewis, B.E. Reus, R.J. Leach, and M. Leppert. 1998. A pore mutation in a novel KQT-like potassium channel gene in an idiopathic epilepsy family. *Nat. Genet.* 18:53–55. <https://doi.org/10.1038/ng0198-53>
- Gao, Z., T. Zhang, M. Wu, Q. Xiong, H. Sun, Y. Zhang, L. Zu, W. Wang, and M. Li. 2010. Isoform-specific prolongation of Kv7 (KCNQ) potassium channel opening mediated by new molecular determinants for drug-channel interactions. *J. Biol. Chem.* 285:28322–28332. <https://doi.org/10.1074/jbc.M110.116392>
- Gonzalez-Perez, V., X.M. Xia, and C.J. Lingle. 2014. Functional regulation of BK potassium channels by γ 1 auxiliary subunits. *Proc. Natl. Acad. Sci. USA*. 111:4868–4873. <https://doi.org/10.1073/pnas.1322123111>
- Gonzalez-Perez, V., X.M. Xia, and C.J. Lingle. 2015. Two classes of regulatory subunits coassemble in the same BK channel and independently regulate gating. *Nat. Commun.* 6:8341. <https://doi.org/10.1038/ncomms9341>
- Gourgy-Hacohen, O., P. Kornilov, I. Pittel, A. Peretz, B. Attali, and Y. Paas. 2014. Capturing distinct KCNQ2 channel resting states by metal ion bridges in the voltage-sensor domain. *J. Gen. Physiol.* 144:513–527. <https://doi.org/10.1085/jgp.201411221>
- Gunthorpe, M.J., C.H. Large, and R. Sankar. 2012. The mechanism of action of retigabine (ezogabine), a first-in-class K⁺ channel opener for the treatment of epilepsy. *Epilepsia*. 53:412–424. <https://doi.org/10.1111/j.1528-1167.2011.03365.x>
- Haley, J.E., F.C. Abogadie, P. Delmas, M. Dayrell, Y. Vallis, G. Milligan, M.P. Caulfield, D.A. Brown, and N.J. Buckley. 1998. The alpha subunit of Gq contributes to muscarinic inhibition of the M-type potassium current in sympathetic neurons. *J. Neurosci.* 18:4521–4531. <https://doi.org/10.1523/JNEUROSCI.18-12-04521.1998>
- Kalappa, B.I., H. Soh, K.M. Duignan, T. Furuya, S. Edwards, A.V. Tzingounis, and T. Tzouanopoulos. 2015. Potent KCNQ2/3-specific channel activator suppresses in vivo epileptic activity and prevents the development of tinnitus. *J. Neurosci.* 35:8829–8842. <https://doi.org/10.1523/JNEUROSCI.5176-14.2015>
- Kim, R.Y., M.C. Yau, J.D. Galpin, G. Seebohm, C.A. Ahern, S.A. Pless, and H.T. Kurata. 2015. Atomic basis for therapeutic activation of neuronal potassium channels. *Nat. Commun.* 6:8116. <https://doi.org/10.1038/ncomms9116>
- Kim, R.Y., S.A. Pless, and H.T. Kurata. 2017. PIP2 mediates functional coupling and pharmacology of neuronal KCNQ channels. *Proc. Natl. Acad. Sci. USA*. 114:E9702–E9711. <https://doi.org/10.1073/pnas.1705802114>
- Lange, W., J. Geissendörfer, A. Schenzer, J. Grötzinger, G. Seebohm, T. Friedrich, and M. Schwake. 2009. Refinement of the binding site and mode of action of the anticonvulsant Retigabine on KCNQ K⁺ channels. *Mol. Pharmacol.* 75:272–280. <https://doi.org/10.1124/mol.108.052282>
- Large, C.H., D.M. Sokal, A. Nehlig, M.J. Gunthorpe, R. Sankar, C.S. Crean, K.E. Vanlandingham, and H.S. White. 2012. The spectrum of anticonvulsant efficacy of retigabine (ezogabine) in animal models: implications for clinical use. *Epilepsia*. 53:425–436. <https://doi.org/10.1111/j.1528-1167.2011.03364.x>
- Li, P., Z. Chen, H. Xu, H. Sun, H. Li, H. Liu, H. Yang, Z. Gao, H. Jiang, and M. Li. 2013a. The gating charge pathway of an epilepsy-associated potassium channel accommodates chemical ligands. *Cell Res.* 23:1106–1118. <https://doi.org/10.1038/cr.2013.82>
- Li, S., V. Choi, and T. Tzouanopoulos. 2013b. Pathogenic plasticity of Kv7.2/3 channel activity is essential for the induction of tinnitus. *Proc. Natl. Acad. Sci. USA*. 110:9980–9985. <https://doi.org/10.1073/pnas.1302770110>
- McCormack, K., L. Lin, L.E. Iverson, M.A. Tanouye, and F.J. Sigworth. 1992. Tandem linkage of Shaker K⁺ channel subunits does not ensure the stoichiometry of expressed channels. *Biophys. J.* 63:1406–1411. [https://doi.org/10.1016/S0006-3495\(92\)81703-4](https://doi.org/10.1016/S0006-3495(92)81703-4)
- Meisel, E., M. Dvir, Y. Haitin, M. Giladi, A. Peretz, and B. Attali. 2012. KCNQ1 channels do not undergo concerted but sequential gating transitions in both the absence and the presence of KCNE1 protein. *J. Biol. Chem.* 287:34212–34224. <https://doi.org/10.1074/jbc.M112.364901>

- Miceli, F., M.V. Soldovieri, M. Martire, and M. Tagliatalata. 2008. Molecular pharmacology and therapeutic potential of neuronal Kv7-modulating drugs. *Curr. Opin. Pharmacol.* 8:65–74. <https://doi.org/10.1016/j.coph.2007.10.003>
- Miceli, F., M.V. Soldovieri, P. Ambrosino, L. Manocchio, A. Medoro, I. Mosca, and M. Tagliatalata. 2018. Pharmacological Targeting Of Neuronal Kv7.2/3 Channels: A Focus On Chemotypes And Receptor Sites. *Curr. Med. Chem.* 25:2637–2660. <https://doi.org/10.2174/0929867324666171012122852>
- Orhan, G., T.V. Wuttke, A.T. Nies, M. Schwab, and H. Lerche. 2012. Retigabine/Ezogabine, a KCNQ/K(V)7 channel opener: pharmacological and clinical data. *Expert Opin. Pharmacother.* 13:1807–1816. <https://doi.org/10.1517/14656566.2012.706278>
- Padilla, K., A.D. Wickenden, A.C. Gerlach, and K. McCormack. 2009. The KCNQ2/3 selective channel opener ICA-27243 binds to a novel voltage-sensor domain site. *Neurosci. Lett.* 465:138–142. <https://doi.org/10.1016/j.neulet.2009.08.071>
- Passmore, G.M., A.A. Selyanko, M. Mistry, M. Al-Qatari, S.J. Marsh, E.A. Matthews, A.H. Dickenson, T.A. Brown, S.A. Burbidge, M. Main, and D.A. Brown. 2003. KCNQ/M currents in sensory neurons: significance for pain therapy. *J. Neurosci.* 23:7227–7236. <https://doi.org/10.1523/JNEUROSCI.23-18-07227.2003>
- Sack, J.T., O. Shamotienko, and J.O. Dolly. 2008. How to validate a heteromeric ion channel drug target: assessing proper expression of concatenated subunits. *J. Gen. Physiol.* 131:415–420. <https://doi.org/10.1085/jgp.200709939>
- Schenzer, A., T. Friedrich, M. Pusch, P. Saftig, T.J. Jentsch, J. Grötzinger, and M. Schwake. 2005. Molecular determinants of KCNQ (Kv7) K⁺ channel sensitivity to the anticonvulsant retigabine. *J. Neurosci.* 25:5051–5060. <https://doi.org/10.1523/JNEUROSCI.0128-05.2005>
- Singh, N.A., C. Charlier, D. Stauffer, B.R. DuPont, R.J. Leach, R. Melis, G.M. Ronen, I. Bjerre, T. Quattlebaum, J.V. Murphy, et al. 1998. A novel potassium channel gene, KCNQ2, is mutated in an inherited epilepsy of newborns. *Nat. Genet.* 18:25–29. <https://doi.org/10.1038/ng0198-25>
- Soldovieri, M.V., P. Ambrosino, I. Mosca, M. De Maria, E. Moretto, F. Miceli, A. Alaimo, N. Iraci, L. Manocchio, A. Medoro, et al. 2016. Early-onset epileptic encephalopathy caused by a reduced sensitivity of Kv7.2 potassium channels to phosphatidylinositol 4,5-bisphosphate. *Sci. Rep.* 6:38167. <https://doi.org/10.1038/srep38167>
- Suh, B.C., and B. Hille. 2007. Regulation of KCNQ channels by manipulation of phosphoinositides. *J. Physiol.* 582:911–916. <https://doi.org/10.1113/jphysiol.2007.132647>
- Suh, B.C., T. Inoue, T. Meyer, and B. Hille. 2006. Rapid chemically induced changes of PtdIns(4,5)P₂ gate KCNQ ion channels. *Science.* 314:1454–1457. <https://doi.org/10.1126/science.1131163>
- Telezkhin, V., A.M. Thomas, S.C. Harmer, A. Tinker, and D.A. Brown. 2013. A basic residue in the proximal C-terminus is necessary for efficient activation of the M-channel subunit Kv7.2 by PI(4,5)P₂. *Pflugers Arch.* 465:945–953. <https://doi.org/10.1007/s00424-012-1199-3>
- Wainger, B.J., E. Kiskinis, C. Mellin, O. Wiskow, S.S. Han, J. Sandoe, N.P. Perez, L.A. Williams, S. Lee, G. Boulting, et al. 2014. Intrinsic membrane hyperexcitability of amyotrophic lateral sclerosis patient-derived motor neurons. *Cell Reports.* 7:1–11. <https://doi.org/10.1016/j.celrep.2014.03.019>
- Wang, A.W., R. Yang, and H.T. Kurata. 2017. Sequence determinants of subtype-specific actions of KCNQ channel openers. *J. Physiol.* 595:663–676. <https://doi.org/10.1113/JP272762>
- Wang, A.W., M.C. Yau, C.K. Wang, N. Sharmin, R.Y. Yang, S.A. Pless, and H.T. Kurata. 2018. Four drug-sensitive subunits are required for maximal effect of a voltage sensor-targeted KCNQ opener. *J. Gen. Physiol.* <https://doi.org/10.1085/jgp.201812014>
- Wang, H.S., Z. Pan, W. Shi, B.S. Brown, R.S. Wymore, I.S. Cohen, J.E. Dixon, and D. McKinnon. 1998. KCNQ2 and KCNQ3 potassium channel subunits: molecular correlates of the M-channel. *Science.* 282:1890–1893. <https://doi.org/10.1126/science.282.5395.1890>
- Wuttke, T.V., G. Seeböhm, S. Bail, S. Maljevic, and H. Lerche. 2005. The new anticonvulsant retigabine favors voltage-dependent opening of the Kv7.2 (KCNQ2) channel by binding to its activation gate. *Mol. Pharmacol.* 67:1009–1017. <https://doi.org/10.1124/mol.104.010793>
- Xiong, Q., H. Sun, and M. Li. 2007. Zinc pyrithione-mediated activation of voltage-gated KCNQ potassium channels rescues epileptogenic mutants. *Nat. Chem. Biol.* 3:287–296. <https://doi.org/10.1038/nchembio874>
- Xiong, Q., Z. Gao, W. Wang, and M. Li. 2008. Activation of Kv7 (KCNQ) voltage-gated potassium channels by synthetic compounds. *Trends Pharmacol. Sci.* 29:99–107. <https://doi.org/10.1016/j.tips.2007.11.010>
- Yu, H., M. Wu, S.D. Townsend, B. Zou, S. Long, J.S. Daniels, O.B. McManus, M. Li, C.W. Lindsley, and C.R. Hopkins. 2011. Discovery, Synthesis, and Structure Activity Relationship of a Series of N-Aryl-bicyclo[2.2.1]heptane-2-carboxamides: Characterization of ML213 as a Novel KCNQ2 and KCNQ4 Potassium Channel Opener. *ACS Chem. Neurosci.* 2:572–577. <https://doi.org/10.1021/cn200065b>
- Zaika, O., C.C. Hernandez, M. Bal, G.P. Tolstykh, and M.S. Shapiro. 2008. Determinants within the turret and pore-loop domains of KCNQ3 K⁺ channels governing functional activity. *Biophys. J.* 95:5121–5137. <https://doi.org/10.1529/biophysj.108.137604>
- Zhou, P., H. Yu, M. Gu, F.J. Nan, Z. Gao, and M. Li. 2013. Phosphatidylinositol 4,5-bisphosphate alters pharmacological selectivity for epilepsy-causing KCNQ potassium channels. *Proc. Natl. Acad. Sci. USA.* 110:8726–8731. <https://doi.org/10.1073/pnas.1302167110>